Electronic Journal of Biotechnology 55 (2022) 78–90

Contents lists available at ScienceDirect

Electronic Journal of Biotechnology

journal homepage:

Research Article

Prognosis prediction ability and prospective biological mechanisms of WDHD1 in hepatocellular carcinoma tissues

Rong-Quan He [a], Jian-Di Li [b], Wei-Ying He [a], Gang Chen [b], Zhi-Guang Huang [b], Ming-Fen Li [c], Wei-Zi Wu [d], Ji-Tian Chen [d], Yan-Qing Pan [b], Huan Jiang [b], Yi-Wu Dang [b], Li-Hua Yang [a,*]

[a] Department of Medical Oncology, First Affiliated Hospital of Guangxi Medical University, No. 6 Shuangyong Rd, Nanning, Guangxi Zhuang Autonomous Region 530021, PR China
[b] Department of Pathology, First Affiliated Hospital of Guangxi Medical University, No. 6 Shuangyong Rd, Nanning, Guangxi Zhuang Autonomous Region 530021, PR China
[c] Clinical Laboratory, The First Affiliated Hospital of the University of Chinese Medicine in Guangxi, No. 89-9 Dongge Road, Nanning, Guangxi Zhuang Autonomous Region 530023, PR China
[d] Department of Pathology, Lingshan People's Hospital, No. 17 Liufeng Rd, Lingshan County, Qinzhou, Guangxi Zhuang Autonomous Region 535400, PR China

GRAPHICAL ABSTRACT

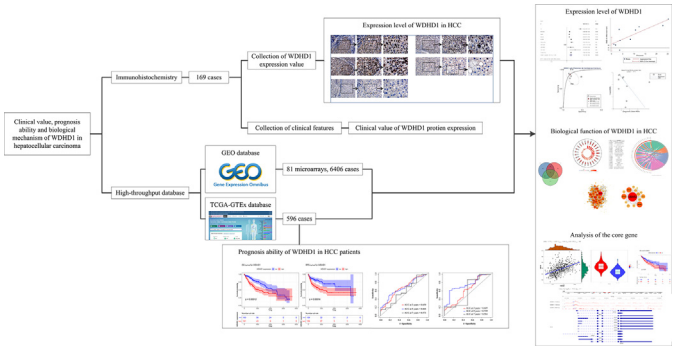

ARTICLE INFO

Article history:
Received 30 May 2021
Accepted 2 December 2021
Available online 8 December 2021

Keywords:
Chromatin immunoprecipitation sequencing
Complex pathogenesis
immunohistochemistry
Gene microarrays
Hepatocellular carcinoma
High-throughput data
High-throughput sequencing
Immunohistochemistry
Liver cancer

ABSTRACT

Background: Hepatocellular carcinoma (HCC) is a malignant tumor with complex pathogenesis. In HCC, the possible roles of transcriptional factor WD repeat and HMG-box DNA binding protein 1 (WDHD1) remain unclear. Hence, our study is aimed at verifying the prognosis prediction ability and potential biological mechanisms of WDHD1 in HCC.

Results: In this study, a total of 7171 clinical samples were obtained to quantitatively analyze the protein and mRNA expression levels of WDHD1 by using immunohistochemistry, gene microarrays, and high-throughput sequencing technologies. The result of in-house immunohistochemistry assay indicated that WDHD1 protein was remarkably overexpressed in HCC tissues compared with the non-HCC tissues (AUC > 0.99, the single Standardized Mean Difference [SMD] = 4.46). The overexpression trend of WDHD1 was validated by the comprehensive analysis based on a total of 4004 HCC tissues and 3167 controls (SMD = 1.333; AUC = 0.91). Moreover, the higher WDHD1 expression resulted in the poorer prognosis of HCC, as assessed by overall survival and relapse-free survival analyses (pooled hazard ratios > 1). WDHD1-coexpressed genes were screened out for enrichment analyses to enquire the prospective signaling pathways of WDHD1 in HCC and to probe the potential transcriptional targets of WDHD1. The

Peer review under responsibility of Pontificia Universidad Católica de Valparaíso
* Corresponding author.
E-mail address: yanglihua_gxmu@163.com (L.-H. Yang).

https://doi.org/10.1016/j.ejbt.2021.12.001

Malignant tumor
Transcription factor
WDHD1

WDHD1-coexpressed genes were mainly involved in the division process of chromosome and cell nucleus in HCC. UBA52 was identified as a crucial target of WDHD1.
Conclusions: WDHD1 may act as an oncogene in HCC and it has the potential to become a novel marker for predicting the prognosis of HCC patients, which may benefit from the early intervention of HCC.
How to cite: He R-Q, Li J-D, He W-Y, et al. Prognosis prediction ability and prospective biological mechanisms of WDHD1 in hepatocellular carcinoma tissues. Electron J Biotechnol 2022;55. https://doi.org/10.1016/j.ejbt.2021.12.001

1. Introduction

Cancer is a growing public problem that affects public health. Liver cancer, a malignant tumor that is increasingly affecting life health (2–3% increase every year), has a low five-year survival rate (18%) worldwide [1,2]. In China, the incidence of liver cancer ranks the fourth among all malignant tumors, and its mortality ranks the second [3]. Hepatocellular carcinoma (HCC) is one of the commonest subtypes of liver cancer, comprising 75–85% of liver cancer cases [4,5]. To date, though there are studies showing that epigenetic changes like DNA methylation [6,7,8,9] may be involved in the progression of HCC, the mechanisms of HCC remain unclear. At the same time, some external factors like hepatitis viral infection, over-drinking, and obesity further add complexity to the pathogenesis of HCC [1,10,11,12]. Thus, the mechanisms of the incidence and development of HCC need further clarification.

The progress of solid tumors is associated with cell proliferation in which DNA replication plays an important role. WD repeat and HMG-box DNA binding protein 1 (WDHD1), located at 14q22.2-q22.3 and possessing a trimeric structure [13], is a transcription factor (TF) closely related to DNA replication [14]. It serves as a platform for the components binding to the replication fork [15]. WDHD1 binds to chromatin, works with the replicative helicase [14], and recruits DNA polymerase [16] to facilitate the start of replication. WDHD1 also serves as an essential intra-S phase checkpoint [17]. The reduction of WDHD1 expression may cause a defective mitosis [18]. As a cancer-related gene, WDHD1 expression is elevated in cervical cancer [19], lung adenocarcinoma [20], cholangiocarcinoma [21], non-small cell lung cancer, and oesophageal squamous cell carcinoma [22]. Previous study has illustrated the pro-survival role of WDHD1 in triple negative breast cancer cells [23]. A recent research has revealed that WDHD1 promotes G1 checkpoint abrogation and may cause human-papillomavirus-related tumors [24]. Moreover, WDHD1 inhibition has been demonstrated to hinder tumor growth and metastasis of cholangiocarcinoma cells [21]. Therefore, there exist intimate associations between WDHD1 and the development of cancer. However, the expression status and possible mechanism of WDHD1 in HCC have been rarely mentioned in previous reports.

Our study comprehensively analyzed the expression value of WDHD1 in HCC based on a large number of human liver samples from both protein and mRNA aspects, which fills the gap in the existing research. The prognosis value of WDHD1 was also appraised in HCC. Moreover, the possible pathways that WDHD1 TF may participate in HCC were also examined by in-silico biological mechanism analyses and protein–protein interaction (PPI) network analysis.

2. Materials and methods

2.1. The clinical value of WDHD1 in HCC

2.1.1. Protein and mRNA expression of WDHD1 in HCC

2.1.1.1. In-house immunohistochemistry (IHC). Samples for IHC were obtained from the tissue microarrays purchased from the Pantomics company. A total of 110 HCC tissues and 59 paratumorous liver tissues were collected. A two-step immunohistochemical technique was adopted. Formalin-fixed and embedded tissues underwent the process of dehydration, the endogenous peroxidase blockage, and the antigens exposure in sequence. Anti-WDHD1 antibody (ab224221, Rabbit polyclonal to WDHD1, Abcam) was the primary antibody at 4°C overnight, and phosphate-buffered saline was used to replace the primary antibody as the control group. Next, the secondary antibody was applied at 25°C for half an hour. Finally, the section was stained with diaminobenzidine, re-stained with haematoxylin, dehydrated and fixed with neutral resin. When extracting the expression of WDHD1, the number of positive cells per 100 cells in each sample was calculated to compare the protein expression value of WDHD1. A method of independent student's t-test and analysis of variance (ANOVA) were done to compare the expression level of WDHD1 for the subgroup analysis of clinical traits. The study protocol was approved by the Ethics Committee of the First Affiliated Hospital of Guangxi Medical University.

2.1.1.2. MRNA expression of WDHD1 in high-throughput databases from HCC samples. The expression value of WDHD1 was obtained from The Cancer Genome Atlas (TCGA) database, GEO (Gene Expression Omnibus) database, ArrayExpress, Sequence Read Archive (SRA), Oncomine, and previous reports. The Genotype-Tissue Expression (GTEx) project was also applied for enlarging the sample size of normal controls for RNA-sequencing data.

From the TCGA and GTEx databases (the following were represented by the TCGA-GTEx database), a total of 371 HCC and 225 controls were downloaded, including the value of WDHD1 expression and corresponding clinical features. Subsequently, the raw count data underwent log transformation.

Other HCC microarrays or RNA-sequencing datasets were searched until Dec 1, 2020 by using the following search terms: hepatocellular carcinoma or HCC. The studies generated were then filtered by using the following requirements: (1) studies must include tissues from HCC and non-HCC patients; (2) WDHD1 value could be extracted; and (3) samples were from humans. Data transformation was the same as what we have described in the last paragraph. Moreover, for a more comprehensive analysis, microarray and high-throughput datasets with the same platform were merged, and the batch effect among different microarrays was subsequently removed. Finally, WDHD1 expression was measured based on the merged datasets above.

2.1.1.3. Comprehensive analysis of WDHD1 expression. When analyzing the expression of WDHD1 in HCC and control samples, in-house IHC and public datasets were combined to enlarge the number of samples for a more comprehensive outcome. To examine the expression level and discriminating ability of WDHD1, the standardized mean difference (SMD) and the area under the curve (AUC) of summary receiver operating characteristic (SROC) curve were calculated by using Stata 15.0 (StataCorp LLC, College Station, TX, USA). The heterogeneity was estimated. A value of I^2 > 50% indicated the existence of significant heterogeneity, and a random

effect model was chosen. Scatter plots and receiver operating characteristic (ROC) curves were drawn by using GraphPad Prism v.8 to visualize the expression levels of WDHD1 in each dataset, and the AUC was applied to evaluate the discriminating ability.

2.1.2. Clinical value and prognosis prediction ability of WDHD1 expression in HCC

Based on the results from IHC and TCGA HCC cohort, the clinical features of each patient were obtained (such as gender, age, vital status, TNM stage, and so on), and the WDHD1 expression value was matched to the different traits. The overall survival (OS) and recurrence-free survival (RFS) data were also acquired from the public HCC cohort datasets. Kaplan–Meier survival and Cox regression analyses were conducted to analyze the prognosis prediction ability of WDHD1 in HCC patients. Moreover, studies from the databases mentioned above with prognosis information were included for the calculation of the pooled hazard ratio (HR), which was necessary to compare the prognosis prediction ability between high and low WDHD1 expression groups. To appraise the prognostic prediction ability of WDHD1 in HCC patients, time-dependent ROC curve with inverse probability of censoring weighting estimation was plotted according to the TCGA HCC cohort. Moreover, risk scores were calculated to predict the prognosis of HCC patients by using the mRNA expression value of WDHD1.

2.2. WDHD1 alternation in HCC

The alternation information of WDHD1 was obtained from cBioPortal. TCGA, PanCancer Atlas dataset was exploited for the analysis, where 366 samples were included. Oncoprint was used to visualize genetic alternations and copy number alternations.

2.3. Screening of the candidate co-expressed genes of WDHD1 for biological functional analysis

The relevant Chromatin Immunoprecipitation sequencing (ChIP-seq) data of WDHD1 were searched from GEO and ENCODE. Potential TF targets with scores $\geq$1 were selected as putative targets of WDHD1, which had been certified by each ChIP-seq study. A total of nine high-throughput datasets were exploited for the screening of the co-expressed genes (CEGs) of WDHD1 and the differentially expressed genes (DEGs). Genes with a correlation coefficient $\geq|\pm 0.4|$ that appeared three times or more in the nine datasets were considered as the CEGs with Pearson's correlation analysis. A Limma package of R was applied for digging out the DEGs. Log2 fold change (logFC) $\geq|\pm 0.4|$ was the threshold for the differential analysis, and genes that emerged in three or more datasets were classified into the DEGs. CEGs with correlation coefficients $\geq$ 0.4 and DEGs with logFC $\geq$0.4 (P < 0.05) indicated positive correlations and upregulated expression trends. On the other hand, CEGs with correlation coefficients < −0.4 and DEGs with logFC <−0.4 (P < 0.05) indicated negative correlations and downregulated expression trends.

Putative targets, CEGs, and DEGs underwent the intersection, and the intersected genes were regarded as the candidate co-expressed genes for the biological analysis of WDHD1 in HCC.

2.4. Biological function of WDHD1 in HCC

The WDHD1 co-expressed genes were sent to the Gene Ontology (GO) annotation and Kyoto Encyclopedia of Genes and Genomes (KEGG) to dig out the enriched pathways of WDHD1 in HCC by using the clusterProfiler package of R. The z-score was calculated by the following formula with the GO plot package of R to infer whether genes were more likely to be upregulated or downregulated in those GO items [25]: zscore $=\frac{(\text{up-down})}{\sqrt{\text{count}}}$ (up: number of the upregulated genes; down: number of the down regulated genes; count: total number of the genes), and the logFC was calculated and regarded as the measurement for the expression level based on the TCGA-GTEx datasets. Moreover, the connective relation of the candidate core genes was calculated by the Search Tool for the Retrieval of Interacting Genes (STRING) database. Cytoscape 3.5.0 was applied to visualize the PPI network. In the network, core genes were the nodes that had the highest degree centrality calculated by using the cytohHubba plugin, and a k-core decomposition was accomplished to display the stable subnetwork where the core gene was identified with the MCODE plugin. Finally, to further confirm the relation between WDHD1 and the core genes, the peak of WDHD1 based on ChIP-seq was visualized by using IGV_2.8.13 [26].

2.5. Statistical analysis

Detailed statistical methods were described above in each step of the study. P < 0.05 was regarded as statistically significant.

3. Results

3.1. Flowchart of current study

Based on immunohistochemistry and public databases, a total of 7171 samples were collected for our study. WDHD1 expression, prognosis prediction ability, and biological mechanism were analyzed.

3.2. The clinical value of WDHD1 in HCC

3.2.1. Expression of WDHD1 in HCC

3.2.1.1. Protein expression of WDHD1 based on in-house IHC. We first examined the protein expression level of WDHD1 in HCC. As compared with non-tumor samples, WDHD1 expression was significantly elevated in HCC (P < 0.001) and the AUC of WDHD1 upregulation was higher than 0.99 (P < 0.001, Fig. 1). The single SMD for WDHD1 protein by in-house IHC was 4.46 (3.89–5.03).

3.2.1.2. Comprehensive analysis of WDHD1 expression in HCC. A total of 4004 HCC samples and 3167 non-tumor samples were obtained from in-house IHC and public datasets. The selection process of the high-throughput datasets was shown in Fig. S1. Seventy-eight microarrays with the same platform were merged into five datasets, as was shown in Table 1. Scatter plots and ROC curves were drawn and all datasets appear with elevated WDHD1 expression and good discriminatory capability for HCC in Fig. 2. The least AUC was 0.6423 from GSE54238. In addition, Fig. S2 presented the external validation of WDHD1 upregulation in HCC tissues compared with non-HCC tissues. Moreover, the comprehensive SMD was calculated including in-house IHC, which further confirmed the upregulation of WDHD1 in HCC compared with the non-tumor samples (SMD = 1.333 with 95% confidence interval 1.001–1.664; Fig. 3A). The random effect model was chosen due to the high heterogeneity (I^2 = 96.3%, $P_{\text{heterogeneity}}$ < 0.001). Egger funnel diagram (P = 0.245, Fig. 3B) and Deek's funnel plot (P = 0.16, Fig. 3C) all indicated that there was no publication bias. Finally, the SROC curve was plotted, and the AUC was 0.91 (95% confidence interval 0.88–0.93) with a sensitivity of 0.87 and a specificity of 0.82 (Fig. 3D, 3E).

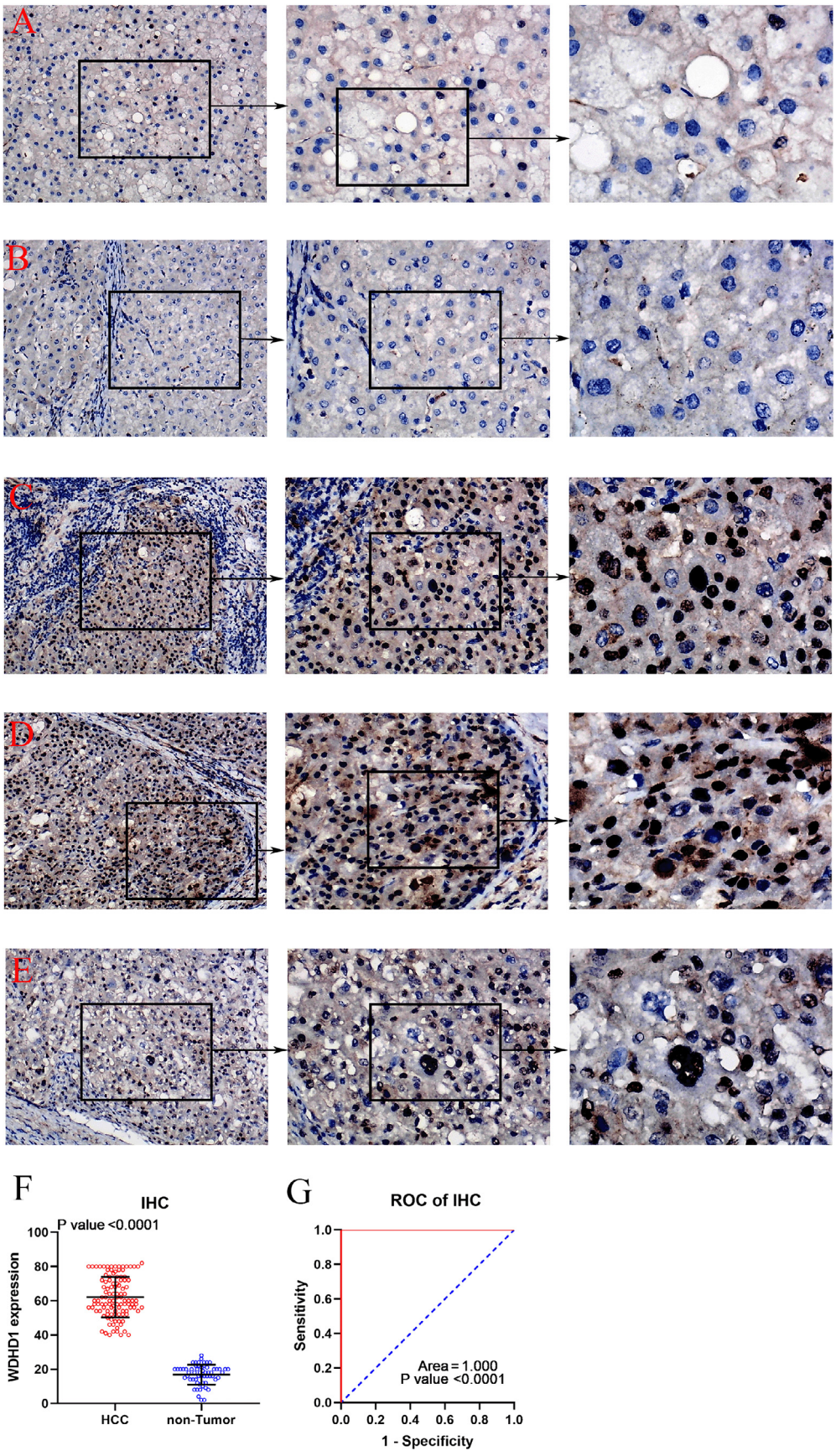

Fig. 1. The expression level of WDHD1 in HCC and non-tumor tissues based on in-house immunohistology. (A and B) Non-tumor tissues (×100, ×200, ×400). (C–E) HCC tissues (×100, ×200, ×400). (F) ROC curve of WDHD1 expression based on TCGA-GTEx database. S, the scatter plot of in-house immunohistochemistry. (G) Receiver operating characteristic curve of WDHD1 expression based on in-house immunohistochemistry.

Table 1
Details of the 5 merged and other 4 high-throughput datasets with corresponding WDHD1 expression level, AUC of the ROC curve, sensitivity and specificity of WDHD1 in HCC.

Datasets	HCC			Non-HCC			ROC		
	N	Mean	SD	*N*	Mean	SD	AUC	Sensitivity	Specificity
Affymetrix	1614	2.921	0.300	1270	2.683	0.176	0.775	0.626	0.787
Agilent	186	2.333	0.272	131	2.094	0.317	0.707	0.812	0.519
Illumina	1278	4.168	0.411	1013	3.854	0.364	0.730	0.623	0.747
Rosetta	368	2.857	0.453	386	2.376	0.179	0.881	0.826	0.793
HiSeq X Ten	38	1.817	0.766	40	0.923	0.221	0.937	0.895	0.850
GSE54238	26	6.092	0.362	30	6.350	0.523	0.642	0.808	0.533
GSE59259	8	7.283	1.008	8	6.302	0.421	0.875	1.000	0.750
GSE74656	5	4.155	0.206	5	3.654	0.160	0.960	1.000	0.800
TCGA-GTEx	371	7.333	1.361	225	5.632	1.032	0.847	0.768	0.822

Note: SD, standard deviation; AUC, area under the curve.
Affymetrix includes GSE101685, GSE102079, GSE107170, GSE112790, GSE121248, GSE12941, GSE14323-GPL571, GSE14520-GPL3921, GSE14520-GPL571, GSE153565, GSE17548, GSE17967, GSE19665, GSE22405, GSE29721, GSE33006, GSE41804, GSE45050, GSE45436, GSE60502, GSE6222, GSE62232, GSE63898, GSE64041, GSE6764, GSE76311-GPL17586, GSE84005, GSE84402, GSE9839, GSE99807.
Agilent includes GSE101728, GSE115018, GSE117361, GSE46408, GSE50579, GSE54236, GSE57555-GPL16699, GSE67764, GSE98269-GPL21047.
Illumina includes GSE104310, GSE112221, GSE20140-GPL18461, GSE25599, GSE31370, GSE33294, GSE36376, GSE36411, GSE39791, GSE46444, GSE55048, GSE56545, GSE57727, GSE57957, GSE63018, GSE63863, GSE65485, GSE69164, GSE73708, GSE76427, GSE77314, GSE77509, GSE81550, GSE87592, GSE87630, GSE89377, GSE94660, GSE97214, GSE98617, GSE102383, GSE102451, GSE138485, GSE140845, GSE144269, GSE154211.
Rosetta includes GSE22058-GPL6793, GSE25097.
HiSeq X Ten includes GSE106830, GSE124535.

3.2.2. Clinical value and prognosis prediction ability of WDHD1 expression in HCC

3.2.2.1. Clinical value of WDHD1 expression. Based on the in-house IHC results, we analyzed the clinical value of WDHD1. WDHD1 expression was notably higher in N1 (72.857 ± 12.212) than N0 stage (61.408 ± 11.516, $P = 0.013$, Table 2), which suggested that despite a weak correlation coefficient, there may be a relationship between the upregulation of WDHD1 and lymph node metastasis ($r = 0.237$, $P = 0.013$).

From the TCGA database, we downloaded the corresponding clinical features of the HCC patients and matched the WDHD1 expression value to see whether there was a difference of expression among various traits. As the result showed in Table 3, patients with advanced T stage, pathological stage, and higher alpha-fetoprotein (AFP) content tended to gain higher WDHD1 expression ($P < 0.05$).

3.2.2.2. Prognosis prediction ability of WDHD1 expression in HCC. The prognosis information was collected from high-throughput datasets. OS and RFS survival curves were drawn based on the datasets from TCGA, which indicated that the higher expression of WDHD1, the poorer prognosis of HCC patients ($P < 0.05$, Fig. 4A, 4B). The pooled HR of the three studies with prognosis information also indicated that patients with a higher WDHD1 expression would possess a poorer prognosis (OS: HR = 1.87, Fig. 4C; RFS: HR = 1.90, Fig. 4D). WDHD1 expression and HBV infection were considered as the two independent factors that influenced the prognosis of HCC patients by Cox regression analysis (Table 4). In addition, the mRNA expression level of WDHD1 displayed a better ability in predicting the 5-year RFS survival probability than the 5-year OS survival probability of HCC patients (Fig. S3A-B). Furthermore, higher WDHD1 mRNA expression level correlated with worse risk scores in HCC patients (Fig. S3C).

3.3. WDHD1 alternation in HCC

The alternation information was downloaded from the cBioPortal website, and as was illustrated by the Oncoprint, there existed missense mutation and amplification in four samples, and most of the samples had the copy-number alternations (Fig. S4).

3.4. Screening of the candidate co-expressed genes and biological functional analyses of WDHD1 in HCC

After the intersection of putative targets of WDHD1 as a TF, its CEGs, and DEGs in HCC, a total of 350 genes were finally included as the candidate core genes related to WDHD1 in HCC (Fig. 5A). In Fig. 5B, the top items ranked by adjusted P value were displayed in the GO-circle plot (the molecular mechanisms only had five items enriched). The outer circle in Fig. 5B showed the level of each gene's logFC value, while the red and blue colors represented the upregulation and downregulation, respectively, which indicated that most of the items in GO had their genes upregulated according to the *z*-score shown in the inner circle. The details of the GO items enriched were shown in Table S1, where ribonucleoprotein complex biogenesis, U2-type spliceosomal complex, and protein N-terminus binding were mostly enriched in the biological process, cellular component, and molecular function, respectively. The result of the KEGG analysis was presented in Fig. 5C and, as the chord plot showed, spliceosome, DNA replication, ribosome, and RNA transport were mostly enriched pathways that appeared in the upregulated trend of the genes included according to the *z*-score. Subsequently, the PPI network was constructed in Fig. 6A, and, ubiquitin A-52 residue ribosomal protein fusion product 1 (UBA52) had the highest degree of centrality, which indicated a close relationship with other genes, which made it the core gene that participated in the regulation of WDHD1 in HCC. Fig. 6B showed the stable structure where UBA52 was involved in the network. As expected, the UBA52 expression was closely related to the WDHD1 expression (Fig. 7A, $r = 0.49$, $P < 0.001$) and was elevated in the HCC samples based on the TCGA-GTEx datasets (Fig. 7B), suggesting that the expression level of UBA52 may be positively modulated by WDHD1 through transcriptional regulation. The higher UBA52 expression also indicated poorer prognosis in HCC patients (Fig. 7C). Finally, the high intensity peak of WDHD1 in the upstream of UBA52 inferred that there existed a binding position of WDHD1 at the promotor of UBA52 (Fig. 7D).

4. Discussion

Based on a large number of samples, our study comprehensively analyzed the WDHD1 expression level in HCC based on in-house IHC and public datasets. We also confirmed that WDHD1 was upregulated in both protein and mRNA levels in HCC patients com-

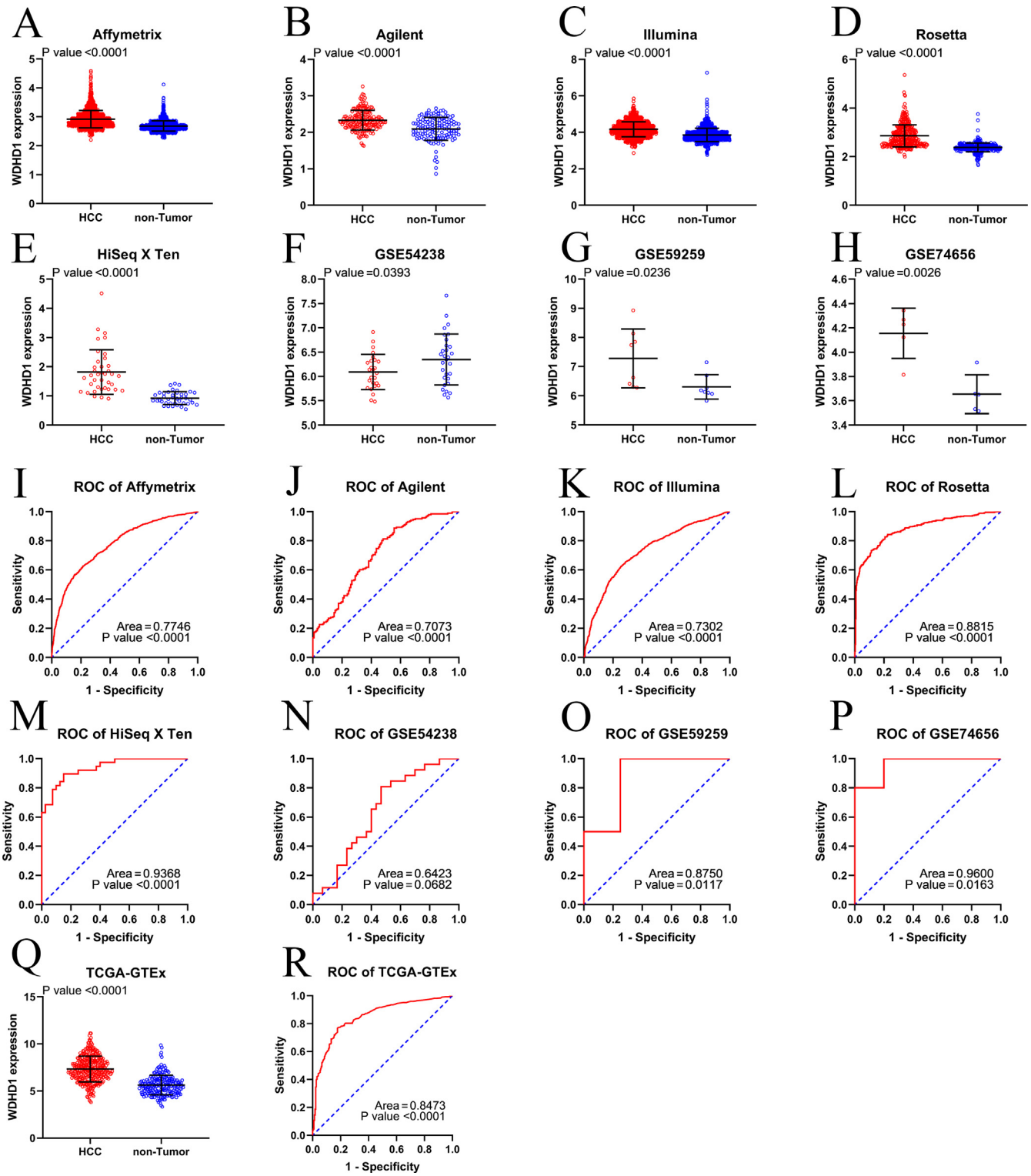

Fig. 2. Expression levels WDHD1 in HCC of all included datasets and in-house immunohistochemistry. (A–H) The scatter plots of the 8 datasets from GEO database. (I–P) Receiver operating characteristic curves of the 8 datasets from GEO database. (Q) The scatter plot of TCGA-GTEx datasets. Most of the datasets appeared the upregulated trend of WDHD1 in HCC compared with the non-HCC tissues and the great discriminating ability of WDHD1 in HCC with AUC >0.7.

pared with the non-HCC samples, which had been rarely reported in previous studies. From the result of clinical value analysis, WDHD1 expression showed strong association with T stage, N stage, pathological stage, and AFP content. Moreover, we confirmed that higher WDHD1 expression was an independent risk factor of the prognosis of HCC patients. Therefore, WDHD1 could be considered as a novel marker for forecasting the prognosis of HCC patients who will benefit from the early intervention. In the aspect of the possible mechanisms of HCC, potential TF targets, CEGs, and DEGs were intersected for the enrichment analysis. It was not surprising that the genes above were involved in the division process of chromosome and cell nucleus, which was in accord

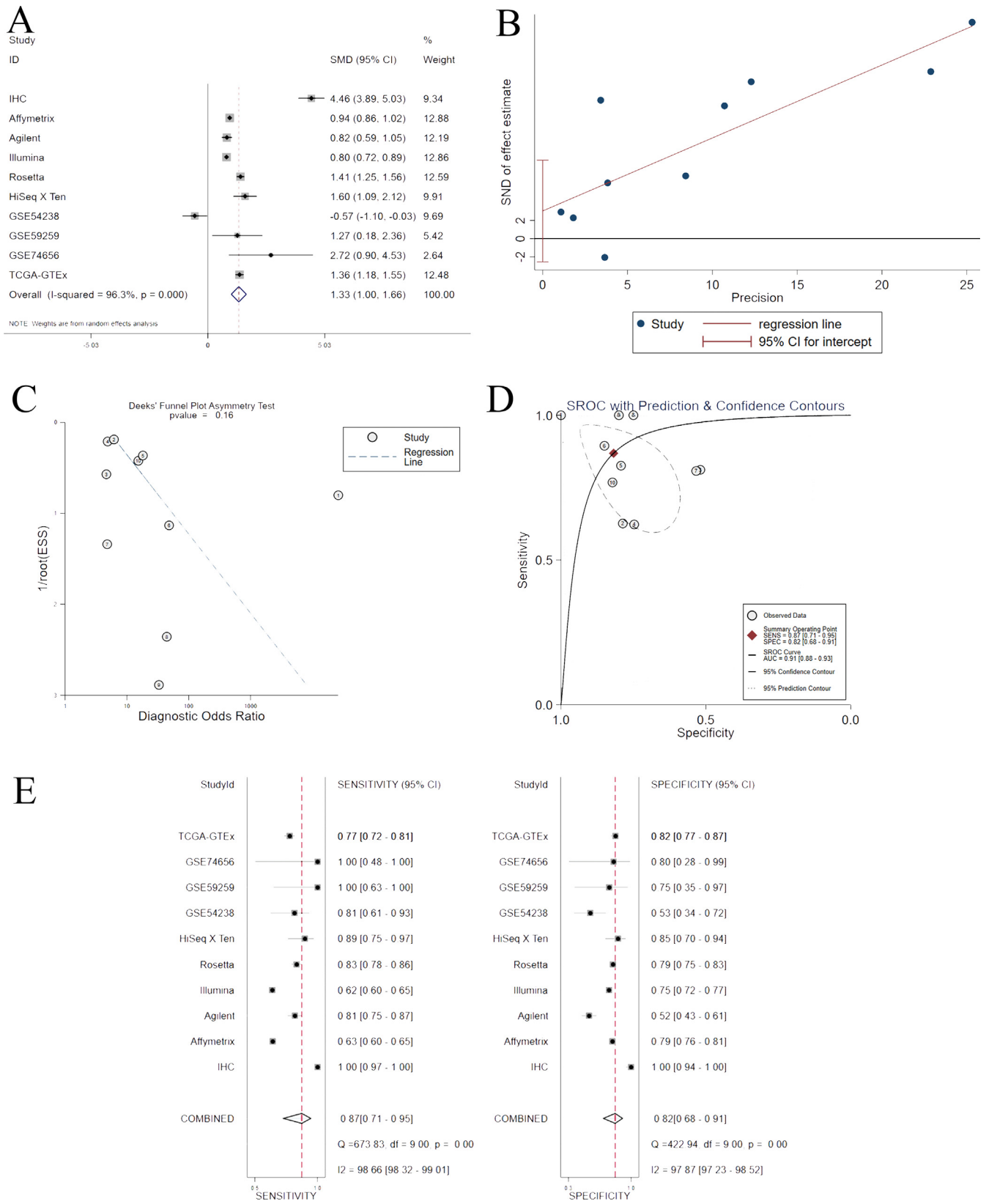

Fig. 3. Comprehensive analysis of the total high-throughput platforms and in-house immunohistochemistry. (A) Forest plot showed that the Standardized mean difference of the total study was >1, which further confirmed the upregulated of WDHD1 in HCC. (B) Egger funnel diagram. $P = 0.245$ indicated little publication bias. (C) Deek's funnel plot. $P = 0.16$ displayed no publication bias. (D) Summary receiver operating characteristic curve was plotted with AUC 0.91 (95% confidence interval 0.88–0.93). (E) Sensitivity and specificity was 0.87 and 0.82, respectively.

Table 2
Clinical value of WDHD1 in HCC based on in-house immunohistochemistry.

Clinicopathological features		WDHD1 expression				
		N	Mean	SD	*P*(*t*)	*t* value
Tissue	non-cancer	59	16.864	5.782	<0.001	27.628
	cancer	110	62.136	11.840		
Gender	male	89	61.483	12.088	0.235	1.193
	female	21	64.905	10.545		
Age	<60	89	61.719	11.846	0.449	0.759
	≥60	21	63.905	11.941		
T stage	T1–T2	81	61.358	11.679	0.251	1.154
	T3–T4	29	64.310	12.221		
N stage	N0	103	61.408	11.516	0.013	2.537
	N1	7	72.857	12.212		
Pathological stage	Stage I–II	81	61.358	11.679	0.224	1.222
	Stage III–IV	28	64.536	12.384		

Table 3
Clinical value of WDHD1 in HCC based on RNA-seq.

Clinicopathological features		WDHD1 expression				
		N	Mean	SD	*P*(*t*)	*t*/*F* value
Tissue	non-cancer	50	5.112	0.875	<0.001	15.593
	cancer	371	7.333	1.361		
Gender	male	250	7.239	1.406	0.056	−1.919
	female	121	7.527	1.246		
Age	<60	169	7.463	1.412	0.091	−1.697
	≥60	201	7.222	1.313		
Vital status	Alive	240	7.173	1.316	0.002	3.122
	Dead	130	7.631	1.402		
T stage	T1–T2	275	7.184	1.303	<0.001	3.852
	T3–T4	93	7.803	1.441		
N stage	N0	252	7.364	1.361	0.206	1.584
	N1	4	8.327	1.454		
	NX	114	7.213	1.343		
M stage	M0	266	7.338	1.363	0.728	0.318
	M1	4	6.793	1.096		
	MX	101	7.341	1.372		
Pathological stage	Stage I–II	257	7.153	1.306	<0.001	3.937
	Stage III–IV	90	7.798	1.42		
Cirrhosis	No	142	7.108	1.341	0.467	0.729
	Yes	70	7.249	1.307		
AFP content	<400	213	7.086	1.286	<0.001	3.777
	≥400	65	7.777	1.305		
HBV Infection	No	248	7.329	1.359	0.977	−0.029
	Yes	104	7.325	1.319		
HCV Infection	No	296	7.359	1.352	0.311	−1.016
	Yes	56	7.16	1.308		
Alcohol Consumption	No	235	7.38	1.305	0.303	−1.032
	Yes	117	7.223	1.424		
Vascular invasion	No	206	7.186	1.257	0.246	1.164
	Yes	109	7.382	1.495		

Note: AFP, alpha-fetoprotein; HBV, hepatitis B virus; HCV, hepatitis C virus.

with the biological behavior of WDHD1 mentioned above. Consequently, we hypothesized that WDHD1 might regulate those target genes and then promote the progress of HCC by facilitating DNA replication, cell division, and proliferation.

We are now facing a critical situation where HCC, a subtype of liver cancer [4], already has a high incidence, high mortality [3], complex mechanism, and multiple limitations of treatment [27,28,29]. Under this situation, precision medicine based on therapeutic targets is proposed to be highly beneficial in the treatment of HCC [30,31]. Thus, more targets should be discovered, and the mechanisms of HCC development need further study. Our study aimed to find more target genes that may be involved in the progress of HCC formation and deterioration and may be helpful in the discriminability, predictive effect of prognosis and even the treatment of HCC patients. WDHD1 has been demonstrated to be a transcription factor participating in DNA replication [14]. As an oncogene, WDHD1 was involved in the formation and progress of multiple tumors. In cervical cancer, WDHD1 is a crucial gene in lymph node metastasis, and the expression was elevated [19]. A recent study reported that WDHD1 could abolish the G1 check-

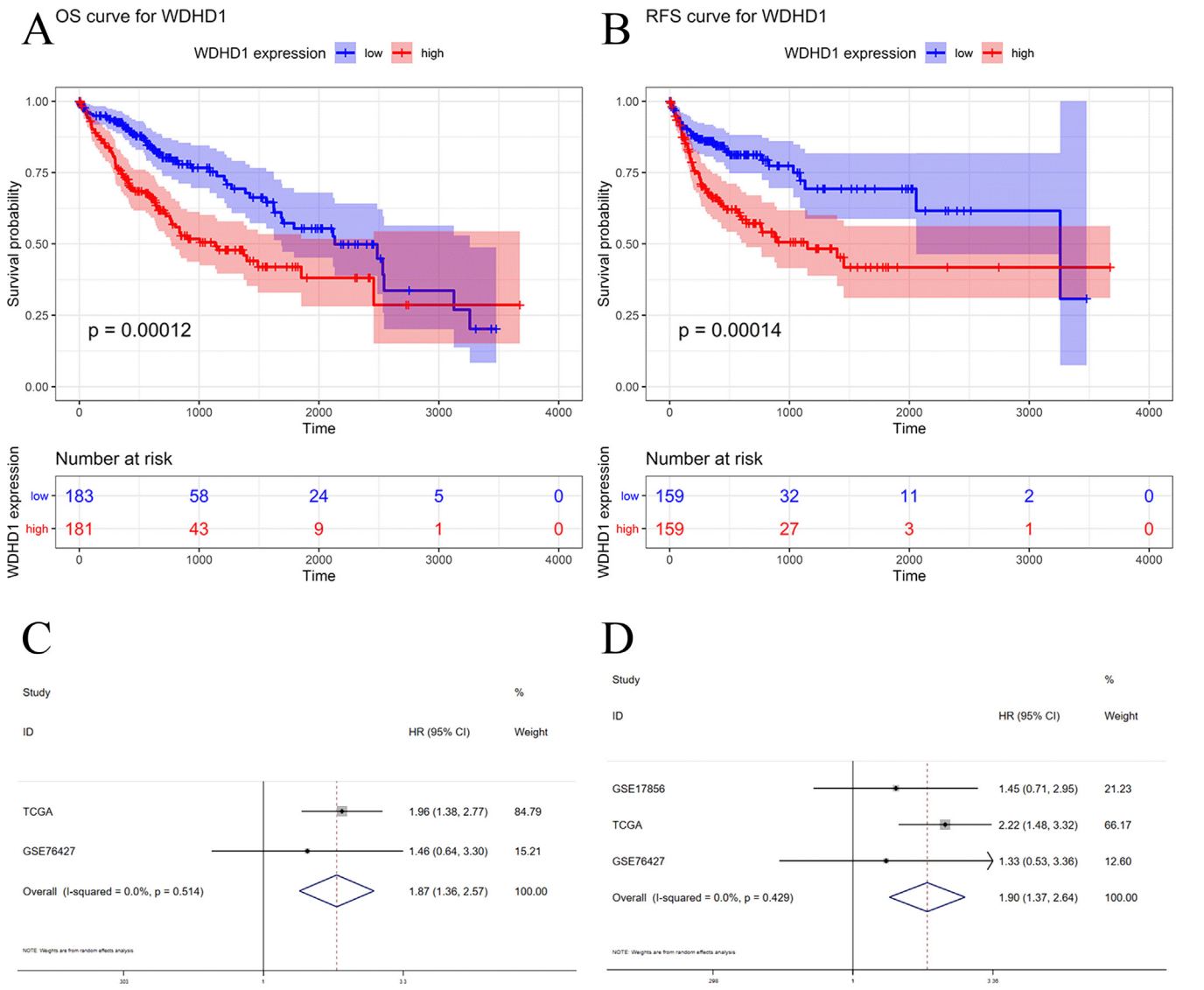

Fig. 4. Kaplan–Meier analysis based of TCGA database and the pooled HR based on total 3 high-throughput datasets. (A) Overall survival (OS) curve. (B) recurrence-free survival (RFS) curve. (C) Pooled HR of overall survival time. (D) Pooled HR of recurrence free survival time. High WDHD1 expression appeared a poorer prognosis.

Table 4
Univariate Cox regression and multivariate Cox regression analysis based on the RNA-seq data.

Characteristics	Univariate Cox regression			Multivariate Cox regression		
	HR	95%CI	*P* value	HR	95%CI	*P* value
WDHD1 expression	1.35	1.183–1.541	<0.001	1.241	1.073–1.435	0.004
Age	1.213	0.855–1.721	0.279	/	/	/
Alcohol consumption	1.025	0.703–1.495	0.898	/	/	/
AFP	1.054	0.644–1.723	0.835	/	/	/
Cirrhosis	0.838	0.479–1.465	0.535	/	/	/
gender	0.817	0.573–1.164	0.263	/	/	/
HBV Infection	0.357	0.221–0.577	<0.001	0.437	0.26–0.735	0.002
HCV Infection	1.09	0.667–1.781	0.732	/	/	/
T stage	2.535	1.782–3.607	<0.001	2.172	0.292–16.161	0.449
M stage	1.275	1.06–1.533	0.01	1.183	0.914–1.531	0.203
N stage	1.223	1.017–1.471	0.032	1.034	0.794–1.345	0.805
Pathologic stage	2.444	1.686–3.543	0	0.889	0.119–6.625	0.909
Vascular invasion	1.35	0.891–2.045	0.157	/	/	/

Note: AFP, alpha-fetoprotein; HBV, hepatitis B virus; HCV, hepatitis C virus.

point that causes genome instability and tumor progression [24]. Similarly, in lung adenocarcinoma, WDHD1 was also closely related to the resistance of cisplatin by promoting the degradation of MAPRE2, which appears to be an upregulated trend of WDHD1 expression [20]. Moreover, in cholangiocarcinoma, WDHD1 expression was upregulated, and the suppression of WDHD1 could

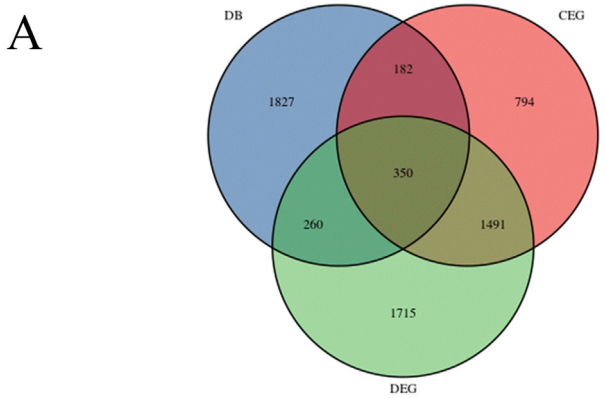

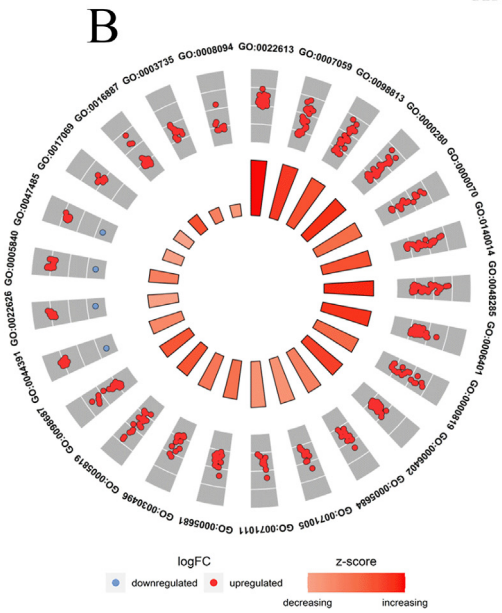

ID	Description
GO:0022613	ribonucleoprotein complex biogenesis
GO:0007059	chromosome segregation
GO:0098813	nuclear chromosome segregation
GO:0000280	nuclear division
GO:0000070	mitotic sister chromatid segregation
GO:0140014	mitotic nuclear division
GO:0048285	organelle fission
GO:0006401	RNA catabolic process
GO:0000819	sister chromatid segregation
GO:0006402	mRNA catabolic process
GO:0005684	U2-type spliceosomal complex
GO:0071005	U2-type precatalytic spliceosome
GO:0071011	precatalytic spliceosome
GO:0005681	spliceosomal complex
GO:0030496	midbody
GO:0005819	spindle
GO:0098687	chromosomal region
GO:0044391	ribosomal subunit
GO:0022626	cytosolic ribosome
GO:0005840	ribosome
GO:0047485	protein N-terminus binding
GO:0017069	snRNA binding
GO:0016887	ATPase activity
GO:0003735	structural constituent of ribosome
GO:0008094	DNA-dependent ATPase activity

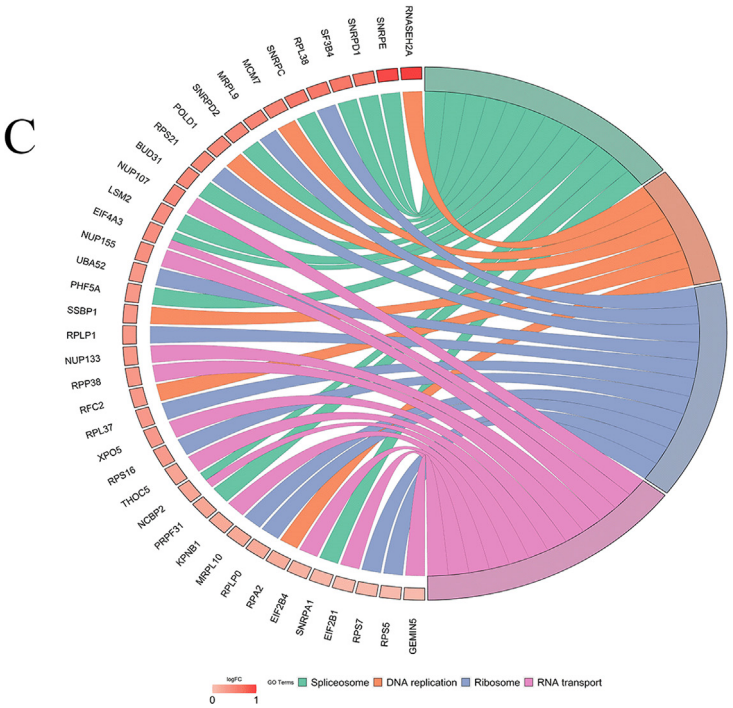

Fig. 5. Potential molecule mechanisms of WDHD1 underlying HCC. (A) The Venn plot displayed the result of the intersection among putative targets, co-expressed genes of WDHD1 and the differentially expressed genes. After the intersection, a total of 350 genes were selected as the candidate core genes. (B) GO-circle plot showed the GO enrichment result of the candidate core genes. The outer circle represented the level of each gene's logfoldchange value, and red color and blue color represented upregulation and downregulation separately. *Z*-score had been shown in the inner circle. The table on the right displayed the Gene Ontology items most enriched. (C) Kyoto Encyclopedia of Genes and Genomes analysis shown by chord plot. Spliceosome, DNA replication, Ribosome and RNA transport were mostly enriched pathways.

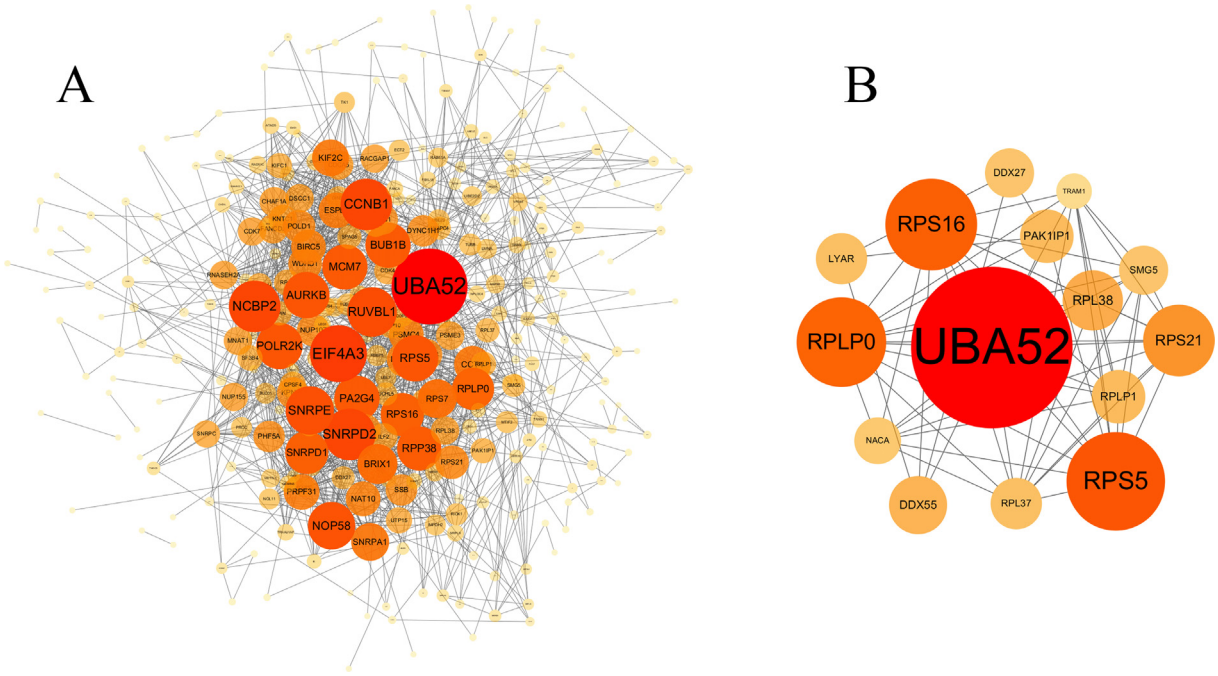

Fig. 6. PPI network construction of 350 intersection genes including WDHD1. (A) PPI of 350 genes. Larger dot size and deeper color represented greater degree centrality. (B) the stable structure that UBA52 involved in the network based on the k-core analysis. PPI, protein-to-protein interaction.

cause cell apoptosis [21]. In another study, WDHD1 was shown to be involved in the phosphoinositide 3-kinase/AKT pathway and was upregulated in non-small cell lung cancer and oesophageal squamous cell carcinomas, where poor prognosis was seen in patients with WDHD1 positive expression. According to this study, the knockout of WDHD1 results in inhibiting cell growth [22]. In conclusion, WDHD1 plays important roles in tumorigenesis, based on the studies presented here. Nevertheless, few studies have reported the expression, clinical value, prognosis, and the mechanisms of WDHD1 in HCC. The current study, for the first time, observed that both of the WDHD1 protein and mRNA expression levels were detected to be evidently upregulated and led to an unfavorable outcome. Surprisingly, WDHD1 has been elucidated as a stage-III-specific upregulated DEGs in HCC [32], which was consistent with the expression and prognostic statuses of WDHD1 in HCC. Moreover, the risk prognostic prediction ability of WDHD1 could be certified by the online result of human protein atlas (https://www.proteinatlas.org/ENSG00000198554-WDHD1/pathology/liver+cancer#ihc) (P = 0.0002). In the present study, The WDHD1 upregulation was validated by multiple cohorts worldwide with a large number of cases of 4004 HCC and 3167 controls, which makes the finding more convincing than those based on a single institute with small sample size. More importantly, multiple detection methods verified the overexpression of WDHD1 in HCC, including in-house immunohistochemistry, microarray, RNA-sequencing, and integrated computational analysis. Therefore, WDHD1 may play an oncogenic role in the incidence and deterioration of HCC.

In this study, we screened out the core co-expressed gene UBA52, which may be a crucial target of WDHD1. Moreover, there is a peak of WDHD1 on the upstream of UBA52, which implies that WDHD1, binding at the promoter of UBA52, regulated the transcription of UBA52 based on the result of ChIP-seq technology. UBA52 was an ubiquitin coding gene located at 19p13.1-p12 [33,34,35,36]. The coding product of UBA52 included ubiquitin and ribosomal protein L40, which promoted the expression of cyclin D, post-translational modification and the formation of ribosomal protein complex [37]. GO and KEGG analysis in our study also revealed that UBA52 participated in the RNA catabolic process, ribosome-related items and pathway. Animal research showed that, in embryos, a deficiency in UBA52 could down-regulate protein expression and result in the cell-cycle arrest [37] and the cessation of embryonic development [38]. In non-small cell lung cancer cells, UBA52-promoting ubiquitination could degrade CCNB1 and then induce cell cloning [39]. We could not help but consider whether WDHD1 could regulate UBA52 and suppress the expression of some crucial genes and contribute to the progress of HCC. In colon cancer and renal cancer, UBA52 expression is an increasing trend [40,41]. With regard to liver cancer, the upregulation of UBA52 could be seen during the apoptosis of the hepatoma cells induced by the anticancer drugs, which caused the gathering of ubiquitylated proteins in the nucleus that was confirmed to be lethal to cells [42]. However, our study showed that UBA52 expression was significantly increased in HCC and higher UBA52 represented poorer prognosis, which seemed to be contradictory to the aforementioned study [42]. As an ubiquitin ligase, the increase expression of WDHD1 would lead to the ubiquitylation and degradation of the specific gene to induce resistance to the cisplatin [20], and UBA52 expression would also increase after applying cisplatin [43]. Thus, we came up with an assumption that WDHD1 might regulate the target gene UBA52 and induce the ubiquitylation of some key genes and against drug-induced apoptosis in HCC, which remains to be verified in further experiments.

Limitations existed in our study. First, larger cohort studies were needed for a more persuasive result for the prognostic value of WDHD1 in HCC. Second, *in vitro* experiments should have been a better method to further verify the results and hypotheses of this study. Last but not least, the subgroup analysis should have been applied to the pre-and post-chemotherapy samples and should have excluded the influence of chemotherapy drugs on the results.

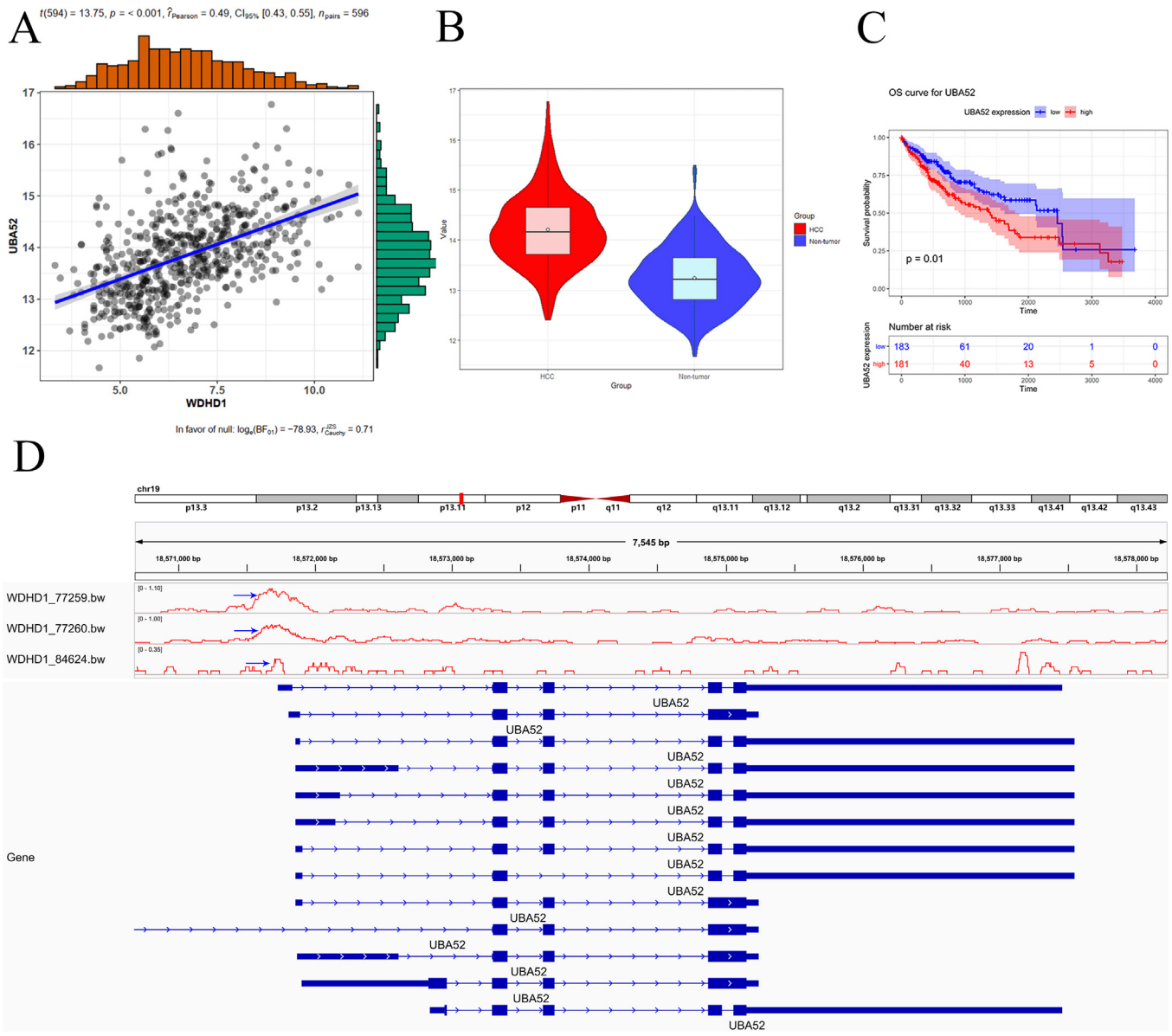

Fig. 7. The analysis of the core gene UBA52. (A) UBA52 expression was closely related to WDHD1 expression. (B) UBA52 expression was elevated in the HCC samples based on the TCGA-GTEx datasets. (C) Higher UBA52 expression indicated poorer prognosis of HCC patients. (D) the high intensity peak of WDHD1 at the upstream of UBA52 inferred that there existed a binding position of WDHD1 at the promotor of UBA52.

5. Conclusions

Our study verified that the elevated expression and prognosis prediction ability of WDHD1 in HCC based on large-scale samples preliminarily clarifying the clinical value of WDHD1. The possible mechanism of WDHD1 in HCC was also inferred, which broadened the horizon for the clarification of the progress and resistance mechanism of HCC and benefits the treatment of HCC patients.

Financial support

This work was supported by Natural Science Foundation of Guangxi, China (2017GXNSFAA198026), Guangxi Zhuang Autonomous Region Health Committee Self-Financed Scientific Research Project (Z20201147, Z20190529, Z20190523), Guangxi Educational Science Planning Key Project (2021), Project funded by China Postdoctoral Science Foundation (No. 2021M693804), Guangxi Higher Education Undergraduate Teaching Reform Project (2020JGA146), Guangxi Medical University Education and Teaching Reform Project (2019XJGZ04), Guangxi Medical University Student Innovation and Entrepreneurship Training Program Project (202010598011, 202010598002), and "Future Academic Star" College Students' Extracurricular Innovation Scientific Research Project (WLXSZX20088).

Conflict of interest

None.

Acknowledgments

We sincerely appreciate the technical support from Guangxi Key Laboratory of Medical Pathology. The authors also appreciate people who contributed to public biomedical databases.

Supplementary data

https://doi.org/10.1016/j.ejbt.2021.12.001.

References

[1] Siegel RL, Miller KD, Jemal A. Cancer statistics, 2020. CA Cancer J Clin 2020;70 (1):7–30. https://doi.org/10.3322/caac.21590. PMid: 31912902.

[2] Cui T, Liu Y, Wang J, et al. Adverse effects of immune-checkpoint inhibitors in hepatocellular carcinoma. OncoTargets Ther 2020;13:11725–40. https://doi.org/10.2147/ott.S279858. PMid: 33235462.

[3] Zheng RS, Sun KX, Zhang SW, et al. Report of cancer epidemiology in China, 2015. Chinese J Oncol 2019;41:19–28. https://doi.org/10.3760/cma.j.issn.0253-3766.2019.01.005. PMid: 30678413.

[4] Bray F, Ferlay J, Soerjomataram I, et al. Global cancer statistics 2018: GLOBOCAN estimates of incidence and mortality worldwide for 36 cancers in 185 countries. CA Cancer J Clin 2018;68(6):394–424. https://doi.org/10.3322/caac.21492. PMid: 30207593.

[5] Shi J, Cao M, Wang Y, et al. Is it possible to halve the incidence of liver cancer in China by 2050? Int J Cancer 2021;148(5):1051–65. https://doi.org/10.1002/ijc.33313. PMid: 32997794.

[6] Fernández-Barrena MG, Arechederra M, Colyn L, et al. Epigenetics in hepatocellular carcinoma development and therapy: The tip of the iceberg. JHEP Rep 2020;2(6):100167. https://doi.org/10.1016/j.jhepr.2020.100167. PMid: 33134907.

[7] Peng JL, Wu JZ, Li GJ, et al. Association of RASSF1A hypermethylation with risk of HBV/HCV-induced hepatocellular carcinoma: A meta-analysis. Pathol Res Pract 2020;216(10):153099. https://doi.org/10.1016/j.prp.2020.153099. PMid: 32853942.

[8] Wang M, Ye Q, Mao D, et al. Research progress in liver-regenerating microenvironment and DNA methylation in hepatocellular carcinoma: the role of traditional Chinese medicine. Med Sci Monit 2020;26:. https://doi.org/10.12659/msm.920310. PMid: 32144233e920310.

[9] Fan X, Jin S, Li Y, et al. Genetic and epigenetic regulation of E-Cadherin signaling in human hepatocellular carcinoma. Cancer Manag Res 2019;11:8947–63. https://doi.org/10.2147/cmar.S225606. PMid: 31802937.

[10] Karakousis ND, Papatheodoridi A, Chatzigeorgiou A, et al. Cellular senescence and hepatitis B-related hepatocellular carcinoma: An intriguing link. Liver Int 2020;40(12):2917–27. https://doi.org/10.1111/liv.14659. PMid: 32890439.

[11] Zeng Z, Yang B, Liao ZY. Current progress and prospect of immune checkpoint inhibitors in hepatocellular carcinoma. Oncol Lett 2020;20:45. https://doi.org/10.3892/ol.2020.11909. PMid: 32802167.

[12] Zhuo JY, Lu D, Tan WY, et al. CK19-positive hepatocellular carcinoma is a characteristic subtype. J Cancer 2020;11(17):5069–77. https://doi.org/10.7150/jca.44697. PMid: 32742454.

[13] Kilkenny ML, Simon AC, Mainwaring J, et al. The human CTF4-orthologue AND-1 interacts with DNA polymerase α/primase via its unique C-terminal HMG box. Open Biol 2017;7(11). https://doi.org/10.1098/rsob.170217. PMid: 29167311.

[14] Li Y, Xiao H, de Renty C, et al. The involvement of acidic nucleoplasmic DNA-binding protein (And-1) in the regulation of prereplicative complex (pre-RC) assembly in human cells. J Biol Chem 2012;287(51):42469–79. https://doi.org/10.1074/jbc.M112.404277. PMid: 23093411.

[15] Rzechorzek NJ, Hardwick SW, Jatikusumo VA, et al. CryoEM structures of human CMG-ATPγS-DNA and CMG-AND-1 complexes. Nucleic Acids Res 2020;48(12):6980–95. https://doi.org/10.1093/nar/gkaa429. PMid: 32453425.

[16] Simon AK, Kummer S, Wild S, et al. The iron-sulfur helicase DDX11 promotes the generation of single-stranded DNA for CHK1 activation. Life Sci Alliance 2020;3(3):e201900547. https://doi.org/10.26508/lsa.201900547. PMid: 32071282.

[17] Yoshizawa-Sugata N, Masai H. Roles of human AND-1 in chromosome transactions in S phase. J Biol Chem 2009;284(31):20718–28. https://doi.org/10.1074/jbc.M806711200. PMid: 19439411.

[18] Hsieh CL, Lin CL, Liu H, et al. WDHD1 modulates the post-transcriptional step of the centromeric silencing pathway. Nucleic Acids Res 2011;39 (10):4048–62. https://doi.org/10.1093/nar/gkq1338. PMid: 21266480.

[19] Chen S, Gao C, Wu Y, et al. Identification of prognostic miRNA signature and lymph node metastasis-related key genes in cervical cancer. Front Pharmacol 2020;11. https://doi.org/10.3389/fphar.2020.00544. PMid: 32457603.

[20] Gong L, Xiao M, He D, et al. WDHD1 leads to cisplatin resistance by promoting MAPRE2 ubiquitination in lung adenocarcinoma. Front Oncol 2020;10. https://doi.org/10.3389/fonc.2020.00461. PMid: 32426268.

[21] Liu B, Hu Y, Qin L, et al. MicroRNA-494-dependent WDHDI inhibition suppresses epithelial-mesenchymal transition, tumor growth and metastasis in cholangiocarcinoma. Dig Liver Dis 2019;51(3):397–411. https://doi.org/10.1016/j.dld.2018.08.021. PMid: 30314946.

[22] Sato N, Koinuma J, Fujita M, et al. Activation of WD repeat and high-mobility group box DNA binding protein 1 in pulmonary and esophageal carcinogenesis. Clin Cancer Res 2010;16(1):226–39. https://doi.org/10.1158/1078-0432.CCR-09-1405. PMid: 20028748.

[23] Ertay A, Liu H, Liu D, et al. WDHD1 is essential for the survival of PTEN-inactive triple-negative breast cancer. Cell Death Dis 2020;11(11). https://doi.org/10.1038/s41419-020-03210-5. PMid: 33221821.

[24] Zhou Y, Pei F, Ji M, et al. WDHD1 facilitates G1 checkpoint abrogation in HPV E7 expressing cells by modulating GCN5. BMC Cancer 2020;20(1). https://doi.org/10.1186/s12885-020-07287-1. PMid: 32883234.

[25] Walter W, Sánchez-Cabo F, Ricote M. GOplot: an R package for visually combining expression data with functional analysis. Bioinformatics 2015;31 (17):2912–4. https://doi.org/10.1093/bioinformatics/btv300. PMid: 25964631.

[26] Busan S, Weeks KM. Visualization of lncRNA and mRNA structure models within the integrative genomics viewer. Methods Mol Biol 2021;2254:15–25. https://doi.org/10.1007/978-1-0716-1158-6_2. PMid: 33326067.

[27] Galle PR, Foerster F, Kudo M, et al. Biology and significance of alpha-fetoprotein in hepatocellular carcinoma. Liver Int 2019;39(12):2214–29. https://doi.org/10.1111/liv.14223. PMid: 31436873.

[28] Scheau C, Badarau IA, Caruntu C, et al. Capsaicin: effects on the pathogenesis of hepatocellular carcinoma. Molecules 2019;24(13):2350. https://doi.org/10.3390/molecules24132350. PMid: 31247901.

[29] Chen S, Cao Q, Wen W, et al. Targeted therapy for hepatocellular carcinoma: Challenges and opportunities. Cancer Lett 2019;460:1–9. https://doi.org/10.1016/j.canlet.2019.114428. PMid: 31207320.

[30] Papatheodoridis GV, Voulgaris T, Papatheodoridi M, et al. Risk scores for hepatocellular carcinoma in chronic hepatitis B: A promise for precision medicine. Hepatology 2020;72(6):2197–205. https://doi.org/10.1002/hep.31440. PMid: 32602980.

[31] Kurebayashi Y, Kubota N, Sakamoto M. Immune microenvironment of hepatocellular carcinoma, intrahepatic cholangiocarcinoma and liver metastasis of colorectal adenocarcinoma: Relationship with histopathological and molecular classifications. Hepatol Res 2021;51 (1):5–18. https://doi.org/10.1111/hepr.13539. PMid: 32573056.

[32] Sarathi A, Palaniappan A. Novel significant stage-specific differentially expressed genes in hepatocellular carcinoma. BMC Cancer 2019;19(1):663. https://doi.org/10.1186/s12885-019-5838-3. PMID: 31277598.

[33] Zhang Y, Zhao H, Xu W, et al. High Expression of *PQBP1* and Low Expression of *PCK2* are associated with metastasis and recurrence of osteosarcoma and unfavorable survival outcomes of the patients. J Cancer 2019;10(9):2091–101. https://doi.org/10.7150/jca.28480. PMid: 31205570.

[34] Wang F, Chen X, Yu X, et al. Degradation of CCNB1 mediated by APC11 through UBA52 ubiquitination promotes cell cycle progression and proliferation of non-small cell lung cancer cells. Am J Transl Res 2019;11(11):7166–85. PMid: 31814919.

[35] Kaur H, Sehgal R, Kumar A, et al. Screening and identification of potential novel biomarker for diagnosis of complicated *Plasmodium vivax* malaria. J Transl Med 2018;16(1). https://doi.org/10.1186/s12967-018-1646-9. PMid: 30286756.

[36] Tomati V, Pesce E, Caci E, et al. High-throughput screening identifies FAU protein as a regulator of mutant cystic fibrosis transmembrane conductance regulator channel. J Biol Chem 2018;293(4):1203–17. https://doi.org/10.1074/jbc.M117.816595. PMid: 29158263.

[37] Kobayashi M, Oshima S, Maeyashiki C, et al. The ubiquitin hybrid gene *UBA52* regulates ubiquitination of ribosome and sustains embryonic development. Sci Rep 2016;6(1). https://doi.org/10.1038/srep36780. PMid: 27829658.

[38] Mao J, O'Gorman C, Sutovsky M, et al. Ubiquitin A-52 residue ribosomal protein fusion product 1 (Uba52) is essential for preimplantation embryo development. Biol Open 2018;7(10):. https://doi.org/10.1242/bio.035717. PMid: 30135083bio035717.

[39] Wei L, Wang X, Lv L, et al. The emerging role of microRNAs and long noncoding RNAs in drug resistance of hepatocellular carcinoma. Mol Cancer 2019;18(1). https://doi.org/10.1186/s12943-019-1086-z. PMid: 31651347.

[40] Barnard GF, Mori M, Staniunas RJ, et al. Ubiquitin fusion proteins are overexpressed in colon cancer but not in gastric cancer. Biochim Biophys Acta – Mol Basis Dis 1995;1272(3):147–53. https://doi.org/10.1016/0925-4439(95)00079-8. PMid: 8541345.

[41] Kanayama H, Tanaka K, Aki M, et al. Changes in expressions of proteasome and ubiquitin genes in human renal cancer cells. Cancer Res 1991;51(24):6677–85. PMid: 1660345..

[42] Han XJ, Lee MJ, Yu GR, et al. Altered dynamics of ubiquitin hybrid proteins during tumor cell apoptosis. Cell Death Dis 2012;3. https://doi.org/10.1038/cddis.2011.142. PMid: 22258406.

[43] Sakai H, Ikeno Y, Tsukimura Y, et al. Upregulation of ubiquitinated proteins and their degradation pathway in muscle atrophy induced by cisplatin in mice. Toxicol Appl Pharmacol 2020;403:115165. https://doi.org/10.1016/j.taap.2020.115165. PMid: 32738330.